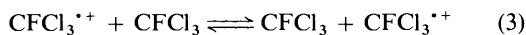
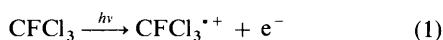


EPR Spectra for a Range of Pyrimidine and *s*-Triazine Radical CationsAidan O'Connell,^a Ian D. Podmore,^a Martyn C. R. Symons,^{*,a} Jane L. Wyatt^a and Franz A. Neugebauer^{*,b}^a Department of Chemistry, The University, Leicester LE1 7RH, UK^b Abt. Organische Chemie, Max-Planck-Institut für medizinische Forschung, Jahnstr. 29, D 6900 Heidelberg, Germany

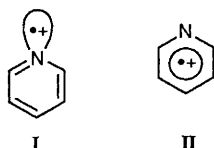
Pyrimidine and *s*-triazine radical cations have been prepared by exposing dilute solutions in freons to ⁶⁰Co γ-rays at 77 K, and studied by EPR spectroscopy. Spectral interpretation is difficult because of the unknown angle (θ) subtended between the principle directions of the ¹⁴N hyperfine axes. Various deuteriated derivatives have been used, together with a range of computer-simulated spectra, which show how the spectra for a two-equivalent-nitrogen system change with θ. From these, the best spectra have been selected for comparison with experiment. The results are discussed in terms of two alternative interpretations offered previously. It is concluded that neither is correct, because of the neglect of weak outer features which are only clearly defined for the 2,4,6-trimethyl *s*-triazine derivative. The new results show that the SOMO is largely concentrated on two nitrogen 'lone-pair' in-plane orbitals with a nodal-surface passing through positions 2 and 5. The estimated p:s ratio on each nitrogen is *ca.* 4.8.

Although radical cations have been studied extensively in the gas phase by a wide range of techniques, and despite early work on liquid-phase species using EPR spectroscopy¹⁻⁵ it is only recently that general procedures have been devised for both liquid-phase⁶⁻¹⁰ and solid-state⁹⁻¹⁹ preparation of these important intermediates. In the present study we have used a general method involving exposure of very dilute solutions of the neutral precursors in various freons to ionizing radiation.^{20,21} The basis of this method is summarized in eqns. (1)–(4) for solvent CFC1₃. The CFC1₃^{•+} cation moves *via* e⁻

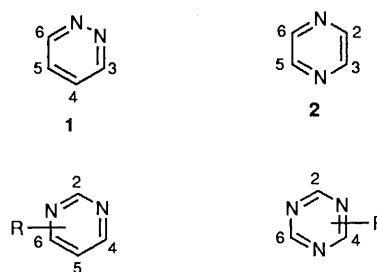


transfer and S^{•+} is formed provided its ionization potential is less than that for CFC1₃. Since the EPR spectrum for [•]CFC1₂ (or possibly CFC1₃^{•-})²² is a single very broad feature at 77 K, this only corresponds to the base-line, and resolved features can be assigned to parent S^{•+} cations or unimolecular products thereof, with confidence.

This procedure was used by Shida and coworkers in the preparation of pyridine radical-cations, whose EPR spectra clearly established the σ-structure I rather than the alternative π-structure II.²³ This work was extended to include various



diazine radical cations¹¹⁻¹³ and substituted derivatives having either σ- or π-SOMOs.^{9,10} Data for some diazine radical cations are included in Table 1. We draw attention to the three sets of rather different results for pyrimidine radical cations. The original data¹¹ for these were clearly unsatisfactory, and two alternative interpretations have been presented.^{11,12}



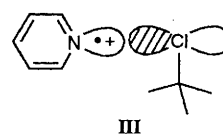
3a; R = H

b; R = 2-²Hc; R = 2,4,5,6-²H₄d; R = 4,6-(CH₃)₂e; R = 2,5-(CH₃)₂

4a; R = H

b; R = 2,4,6-²H₃c; R = 2,4,6-(CH₃)₃

The unusual form of the EPR spectra, and the small values for the ¹⁴N hyperfine splittings led one of us to propose that only one nitrogen contributed to the spectrum. This requires a distortion induced by the medium, which could, for example, involve weak bonding with one chlorine of a solvent molecule as in III. Such bonding often occurs,²⁴ but generally



hyperfine coupling to chlorine is detectable. Shida and coworkers later showed¹³ that this concept must be wrong, because the deuteriated derivative, [2-²H]pyrimidine (3b), gave an EPR spectrum identical with that of the parent compound. {We had also studied this derivative, together with the perdeuteriated form, [2,4,5,6-²H₄]pyrimidine (3c), and came to the same conclusion}. However, as shown below, we still had reservations about the best method of interpreting the complex EPR spectra. The revised data of Shida and coworkers¹³ also given in Table 1 still suggest that the ¹⁴N hyperfine splittings are very small relative to those for the other diazines. No

Table 1 EPR hyperfine parameters for diazine radical cations $1^{+\bullet}$, $2^{+\bullet}$ and $3a^{+\bullet}$ in freon

Radical cation	N_i	HFC/G ^a				$\theta/^\circ$	
		<i>x</i>	<i>y</i>	<i>z</i>	<i>iso</i>		
$1^{+\bullet b}$	N(1,2)	53.5	51.5	65.5	12.6	4	
	H(3,6)						-3.0
	H(4,5)						
$2^{+\bullet b}$	N(1,4)	18.4	18.4	32.7	30.6		
	H(2,3,5,6)						
$3a^{+\bullet c}$	N(1,3)	6.1	25.8	7.0	9.7		
	H(2)	8.6	4.9	4.4			
	H(4,6)	29.7	26.6	26.2			
	H(5)	5.1	0.0	-1.5			
$3a^{+\bullet d}$	1N	28	60	28	ca. 28		
	2H						
	1H						ca. 12
	1H						ca. 8
$3a^{+\bullet b}$	N(1,3)	11.0	10.0	29.5	0.2	68	
	H(2)						29.3
	H(4,6)						
	H(5)						

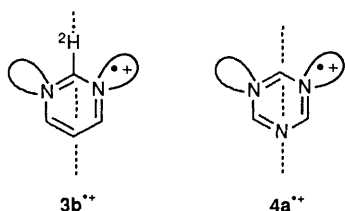
^a 1 G = 10⁻⁴ T. ^b Ref. 13. ^c Ref. 11. ^d Ref. 12.

Table 2 Present EPR hyperfine parameters for various pyrimidine and *s*-triazine radical cations in CFCl₃

Radical cation	¹ H (2) HFC/G ^a		¹⁴ N (2) HFC/G		$\theta/^\circ$
	<i>iso</i>			⊥	
$3a^{+\bullet}$	29		58	23	22 or 68
$3b^{+\bullet}$	29		58	23	
$3c^{+\bullet}$			58	23	22 or 68
$3d^{+\bullet}$			58	23	
$3e^{+\bullet}$	30		57	22	22 or 68
$4a^{+\bullet}$	28		63	42	
$4b^{+\bullet}$			63	42	
$4c^{+\bullet}$			63	42	

^a 1 G = 10⁻⁴ T.

explanation for this apparent anomaly was offered. The reason why the spectrum was unchanged for the deuteriated $3b^{+\bullet}$ is because the SOMO has a nodal surface through the two C-H units (---) as indicated in $3b^{+\bullet}$.



A similar SOMO is expected for the symmetrical triazine (1,3,5-triazine) ($4a^{+\bullet}$). Thus the EPR spectrum for the σ -radical cation should show hyperfine coupling of two equivalent ¹⁴N nuclei, coupling to the third being very small. (The resulting cation is expected to distort to stabilize this structure: the three nitrogens could appear to be equivalent if this distortion were to be dynamic on the EPR time-scale, but this does not occur so far as we can judge.) A brief note on the EPR spectrum for the *s*-triazine cation gave an interpretation involving a single ¹⁴N contribution, based on the distortion concept for the pyrimidine cation.²⁵ Again, although the form of the spectrum seems to

favour this interpretation, we suggest herein that this is misleading.

The aim of the present study was two-fold. One was to probe the concept of a distorted cation with only one strongly coupled ¹⁴N nucleus, and the other was to try to explain the reason for the unusual hyperfine splittings, given that the pyrimidine and *s*-triazine cations are symmetrical.

Experimental

The pyrimidines $3a$ and $3d$ and the *s*-triazines $4a$ and $4b$, obtained commercially, were purified by chromatography on silica gel and subsequent distillation. [2-²H]-($3b$) and [2,4,5,6-²H₄]-pyrimidine ($3c$) were obtained by [²H₂]hydrogenation of 2-chloro- and 2,4,5,6-tetrachloropyrimidine as described in the literature,^{26,27} and also 2,5-dimethylpyrimidine ($3e$)²⁸ and 2,4,6-trimethyl-*s*-triazine ($4c$)²⁹ were prepared by known methods.

For the freon studies, very dilute solutions in CFCl₃ ($\leq 1:1000$) were deoxygenated, and frozen as small beads in liquid nitrogen. The freon was purified by passage through an alumina column. Solutions were irradiated at 77 K in a ⁶⁰Co Vickrad γ -ray source for doses of a few hundred rad. EPR spectra of these irradiated samples were measured on a Varian E 109 spectrometer at 77 K. Samples were annealed by decanting the coolant from the insert Dewar flask, and allowing the sample to warm while continuously monitoring the spectra. Samples were recooled to 77 K for measurement.

Results and Discussion

s-Triazines.—The compounds studied are listed in Tables 1 and 2, together with the new EPR parameters that we have derived. Typical EPR spectra for pyrimidine radical cations are shown in Fig. 1. For *s*-triazines the best spectrum was that of 1,3,5-trimethyl-*s*-triazine radical cation ($4c^{+\bullet}$), which is presented in Fig. 2 together with a simulation based on the data in Table 2. Apart from features marked β in Fig. 2(a) the fit is good. We were never able to eliminate features β , nor could we reproduce them properly by varying the simulation parameters. However their relative intensities varied considerably in different preparations and they were lost reversibly on warming, so we suggest that they are from an unknown impurity that also forms a radical cation. There can be no doubt that the outermost features in this spectrum are a property of the parent radical cation. They are well accommodated in the simulation, the ¹⁴N hyperfine parameters are now in good accord with expectation compared with the other diazines, and all the features assigned to the cation decay together on annealing.

The spectrum for the *s*-[2,4,6-²H₃]triazine radical cation ($4b^{+\bullet}$) gave almost identical parameters, but the features were less well defined because of hyperfine splitting from two equivalent deuterons. Knowing these data, the spectrum for the parent *s*-triazine radical cation has been reinterpreted as indicated in Table 2.

Pyrimidines.—If the spectrum in Fig. 1 is compared with that in Fig. 2, there is good agreement provided that the outer lines indicated in Fig. 1 are included as part of the spectrum. A study of the spectra for the parent compound, the partially deuteriated compound, and various methyl derivatives shows that similar outer features are always present. Because they are poorly defined relative to the central features, these outer features have previously been ignored by ourselves and other workers. Provided they are included, the EPR parameters prove to be far closer to those for the 1,2-diazine, and also, as expected, to those for the *s*-triazines.

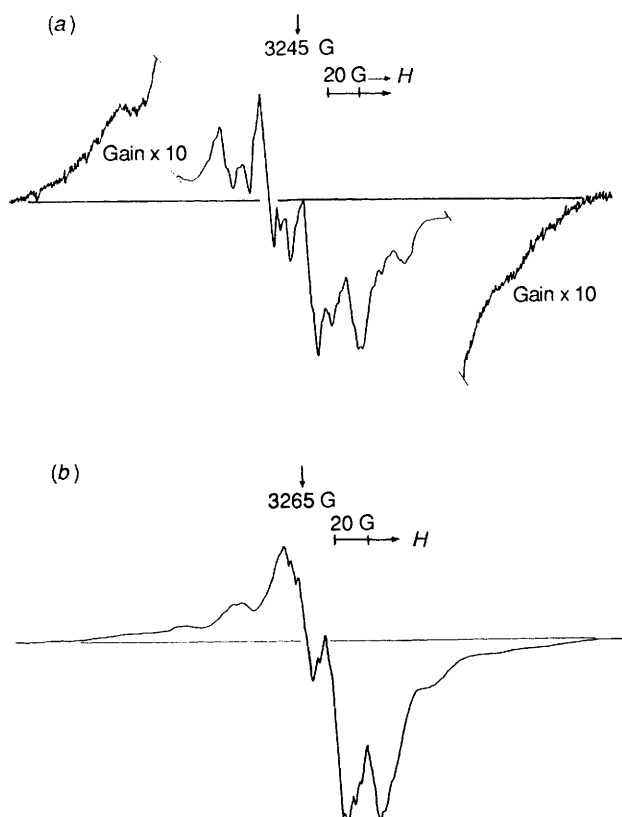


Fig. 1 First derivative X-band EPR spectra for dilute solutions of (a) [2- ^2H]pyrimidine (**3b**) and (b) [2,4,5,6- $^2\text{H}_4$]pyrimidine (**3c**) in CFCl_3 after exposure to ^{60}Co γ -rays at 77 K, showing features assigned to the corresponding radical cations. Note the outer features indicated, which have previously been neglected.

Relative Orientation of ^{14}N Tensor Directions.—Because of the reduced symmetry of these σ -radical cations, the principle directions of the ^{14}N tensors and of the g tensor do not coincide, except for the x direction. This is shown in Fig. 3, which defines the angles used. Instead of simply using a guessed set of angles and computing spectra to give a good fit, we decided to plot spectra for a range of hyperfine coupling constants over a range of angles. Using these, we were at once able to fix the approximate data needed, and then to obtain the best fit shown in Fig. 2(b). These sets of spectra, a selection of which are shown in Fig. 4, are discussed below. We feel that they may be of general use, since they illustrate how spectra vary with angle, and what are the salient features that reveal that the tensors are not coaxial, as is so often assumed.

The best value of θ for all these cations is either *ca.* 22° or *ca.* 68° . The larger value accords well with calculations.^{30,31}

Variation of EPR Spectra for a System with two Equivalent Nuclei having $I = 1$, as a Function of the Angle between the Directions of the Principal Values of the Hyperfine Coupling.—We consider systems in which $g_x = g_y = g_z$ with one hyperfine coupling axis common (A_x). For convenience, we have used axial symmetry, with $A_{\text{max}} = A_{\parallel}$ and $A_{\text{min}} = A_{\perp}$. Also, we have kept A_{\parallel} constant, and used a range of A_{\perp} values. From these we have selected one set when A_{\perp} is large, typical of the σ -radicals discussed above [Fig. 4(a)] and in the other, A_{\perp} is small, being typical of radicals that use only 2p orbitals for the SOMO [Fig. 4(b)].

The sets of spectra show how variation of the angle (θ) causes changes in the spectra. For $\theta = 0^\circ$ or 90° , which is the normal situation considered in spectral analysis, all axes are aligned, and measurement of A_{\parallel} and A_{\perp} for the $M_1 = \pm 2$, ± 1 and 0

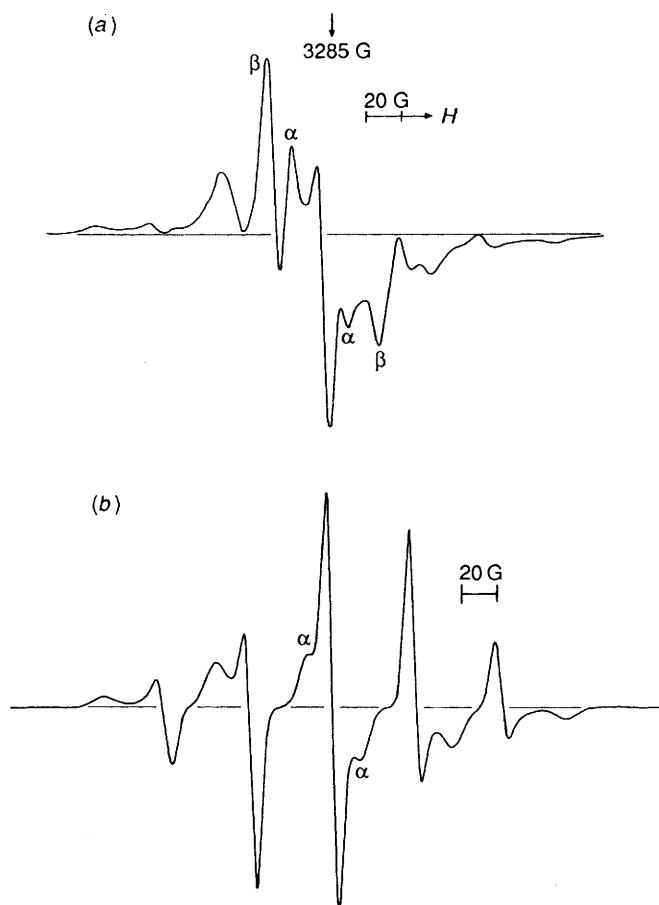


Fig. 2 (a) First-derivative X-band EPR spectrum for a dilute solution of 2,4,6-trimethyl-*s*-triazine (**4c**) in CFCl_3 after exposure to ^{60}Co γ -rays at 77 K, showing features assigned to the corresponding radical cation. (b) Simulation using data from Table 2. [Note the extra lines (β) discussed in the text.]

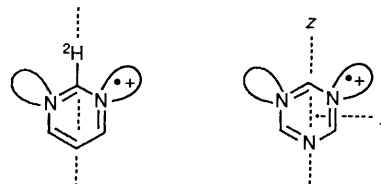


Fig. 3 Coordinates used for simulations

components follows the usual procedure. For θ values between these limits there are systematic changes discussed below. $\theta = 45^\circ$ is the limiting case, and spectra between 0° and 45° are equivalent to those between 90° and 45° . We discuss the empirical changes for cases (a) and (b) and then give brief, qualitative explanations for the changes. We are greatly indebted to Prof. Philip H. Rieger for giving us his programme for these simulations.³²

In case (a) looking at the group of spectra the most noticeable fact is that the ' $M_1 = \pm 1$ ' features do not move from their original positions ($\theta = 0^\circ$). (These labels are used to link with the $\theta = 0^\circ$ case, for convenience.) They also retain their original relative intensities, whilst other features, especially the central $M_1 = 0$ line, have reduced intensities. As θ increases, extra turning-point features appear on either side of the central line (α in Fig. 4). These move out, and in several cases are lost beneath the $M_1 = \pm 1$ lines. The other noteworthy change is that the outermost lines, whilst still resembling the $M_1 = \pm 2$ parallel (z) features, move in steadily towards the mid-point between the

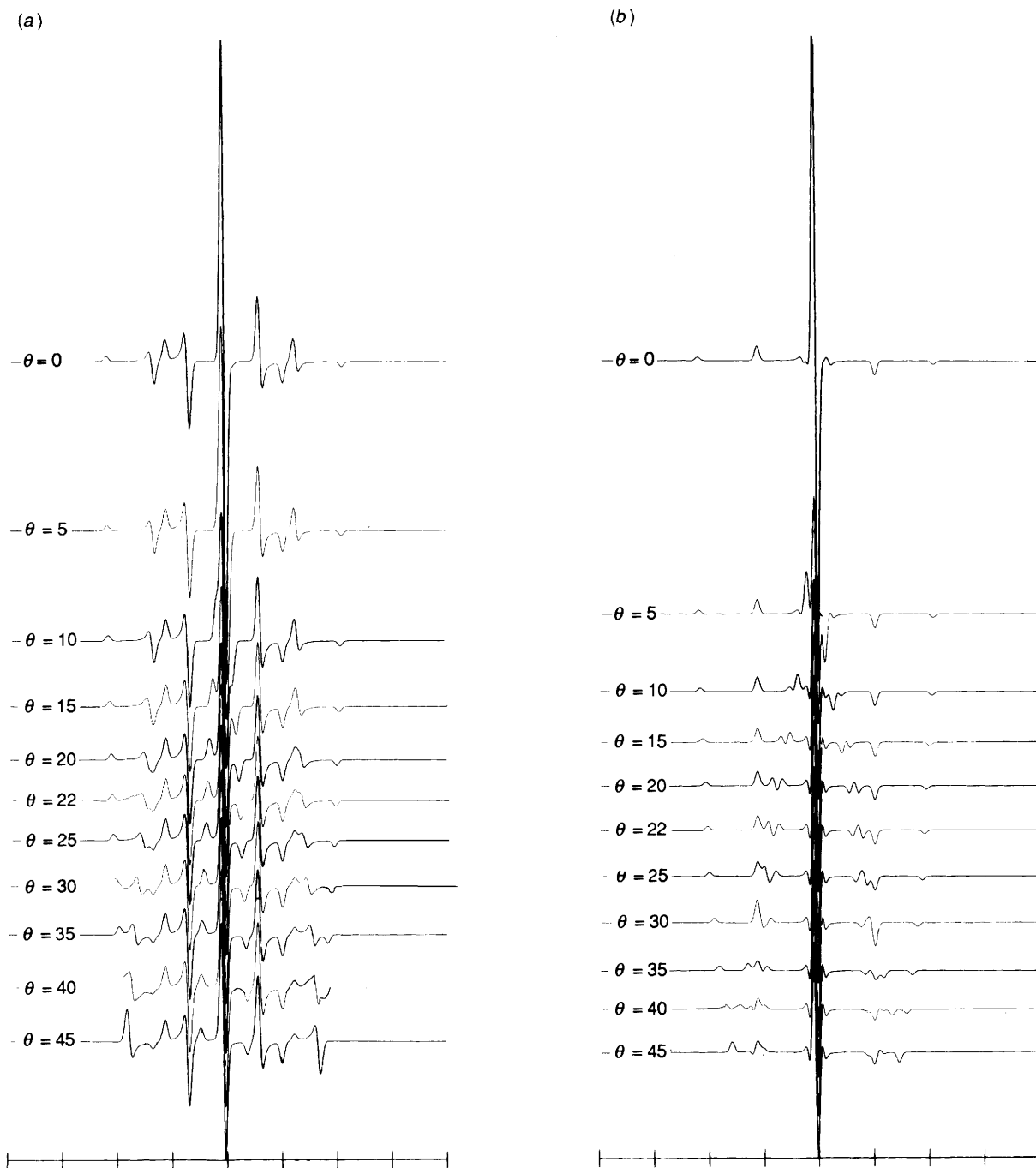


Fig. 4 Sets of simulated EPR spectra for two equivalent ^{14}N nuclei sharing one common axis (x): (a) $A(^{14}\text{N})_{\parallel} = 50 \text{ G}$, $A(^{14}\text{N})_{\perp} = 30 \text{ G}$; (b) $A(^{14}\text{N})_{\parallel} = 50 \text{ G}$, $A(^{14}\text{N})_{\perp} = 5 \text{ G}$. The calibration is in units of 50 G.

original \parallel and \perp components. One of the \perp contributions (the x feature) remains in the original position, while the y feature moves equally with the z feature, until they meet at the mid-way position, giving an apparent perpendicular line. This is characteristic of the $\theta = 45^\circ$ limit. Just such a situation was recently seen for a two ^{31}P σ -type radical.³³ Thus the features to look for are: (i) intense ± 1 lines, which give the two A_{\parallel} and A_{\perp} components directly; (ii) a relatively weak $M_1 = 0$ line; (iii) intermediate lines (x); (iv) a splitting of the $M_1 = \pm 2$ component into three, such that the z and y features move together relative to expectation based on the ± 1 lines. Fitting the ± 2 lines by simulation then gives a good value for θ . The essential reason for the constancy of the ± 1 lines is that they arise from cases in which either N(1) or N(2) have $M_1 = 0$. Hence the second nitrogen can be ignored, and the turning points occur

just as if only one nitrogen were present. Experimentally, care must be taken not to interpret experimental spectra for species with θ between 0° and 45° as arising from just one coupled nitrogen nucleus. The outermost features may be weak, and hence overlooked, whilst the x feature may be concealed by the more intense ± 1 features. Just this situation led to the tentative suggestion that, for the radical cation of pyrimidine, there was a solvent-induced distortion which placed most of the spin density on one nitrogen.¹² The work of Shida *et al.*¹³ and our own studies with deuteriated samples, have shown that this interpretation was indeed incorrect. One of the x features stems from the $M_1 = 0$ line for cases in which one ^{14}N is ± 1 whilst the other is ∓ 1 .

When the difference between A_{\parallel} and A_{\perp} is very large, as is the case for 2p-orbital population, the situation moves to a

dominance of the symmetry axes, and it is necessary to use the squared hyperfine parameters in obtaining averages. The α lines now approach the intensity $M_1 = \pm 1$ (\parallel) lines, and the $y + z$ outer lines do not combine to a single 'perpendicular' feature. Again, care is needed to recognize that this can occur for $\theta = 45^\circ$, but, provided the ± 1 lines can be picked out, this should emerge from simulations.

Conclusions

We conclude that the poorly defined outer features observed for all the pyrimidine and *s*-triazine radical-cation EPR spectra, which have previously been neglected, are part of the spectra. They fit in well with computer reconstructions, giving hyperfine parameters that are in good accord with expectation, and they are lost on annealing, together with the stronger central features.

If this is correct, by matching the spectra with those obtained by computer simulation for a range of values of θ , a best value of 68° is obtained, in good accord with theory. The SOMO is largely confined to two nitrogen orbitals, the p:s ratio estimated from the ^{14}N hyperfine couplings being *ca.* 4.8.

Acknowledgements

We thank Prof. Dr. Philip H. Rieger for giving us his simulation programme and for very helpful discussions.

References

- 1 S. I. Weissman, *J. Chem. Phys.*, 1957, **26**, 963.
- 2 A. Carrington, F. Dravnieks and M. C. R. Symons, *J. Chem. Soc.*, 1959, 947.
- 3 R. Hulme and M. C. R. Symons, *J. Chem. Soc.*, 1965, 1120.
- 4 A. Carrington and J. Dos-Santos-Veiga, *Mol. Phys.*, 1962, **5**, 285.
- 5 J. R. Bolton, A. Carrington and A. D. MacLachlan, *Mol. Phys.*, 1962, **5**, 31.
- 6 D. V. Avila, A. G. Davies, M. L. Girbal and K. M. Ng, *J. Chem. Soc., Perkin Trans. 2*, 1990, 1693.
- 7 D. V. Avila and A. G. Davies, *J. Chem. Soc., Perkin Trans. 2*, 1991, 1111.
- 8 S. F. Nelsen, J. A. Thompson-Colon, B. Kirste, A. Rosenhouse and M. Kaftory, *J. Am. Chem. Soc.*, 1987, **109**, 7128.
- 9 H. Fischer, T. Müller, I. Umminger, F. A. Neugebauer, H. Chandra and M. C. R. Symons, *J. Chem. Soc., Perkin Trans. 2*, 1988, 413.
- 10 U. Eiermann, F. A. Neugebauer, H. Chandra, M. C. R. Symons and J. L. Wyatt, *J. Chem. Soc., Perkin Trans. 2*, 1992, 85.
- 11 Kato and T. Shida, *J. Am. Chem. Soc.*, 1979, **101**, 6869.
- 12 D. N. R. Rao, G. W. Eastland and M. C. R. Symons, *J. Chem. Soc., Faraday Trans. 1*, 1985, **91**, 727.
- 13 M. Matsushita, T. Momose, T. Kato and T. Shida, *Chem. Phys. Lett.*, 1989, **161**, 461.
- 14 F. Williams, Q.-X. Guo, P. A. Petillo and S. F. Nelsen, *J. Am. Chem. Soc.*, 1088, **110**, 7887.
- 15 S. Dai, R. S. Pappas, G.-F. Chen, Q.-X. Guo, J. T. Wang and F. Williams, *J. Am. Chem. Soc.*, 1989, **111**, 8759.
- 16 A. Arnold and F. Gerson, *J. Am. Chem. Soc.*, 1990, **112**, 2027.
- 17 T. Shida, E. Haselbach and T. Bally, *Acc. Chem. Res.*, 1984, **17**, 180.
- 18 L. B. Knight, *Acc. Chem. Res.*, 1986, **19**, 313.
- 19 J. L. Courtneidge and A. G. Davies, *Acc. Chem. Res.*, 1987, **20**, 90.
- 20 M. C. R. Symons, *Chem. Soc. Rev.*, 1984, **13**, 393.
- 21 M. Shiotani, *Magn. Reson. Rev.*, 1987, **12**, 333.
- 22 T. Clark, A. Hasegawa and M. C. R. Symons, *Chem. Phys. Lett.*, 1984, **116**, 79.
- 23 T. Shida and T. Kato, *Chem. Phys. Lett.*, 1979, **68**, 106.
- 24 M. C. R. Symons and J. L. Wyatt, *J. Chem. Res. (S)*, 1989, 362.
- 25 C. J. Rhodes, *J. Chem. Res. (S)*, 1989, 76.
- 26 J. Hervieu, M.-F. Laute-Mouneyrac, J. Dagaut, P. Dizabo, L. C. Leitch and R. N-Renaud, *J. Labelled Comp.*, 1972, **8**, 365.
- 27 F. Milani-Nejad and H. D. Stidham, *Spectrochim. Acta, Part A*, 1975, **31**, 1433.
- 28 R. Kruse and E. Breitmaier, *Chem. Ztg.*, 1977, **101**, 305.
- 29 F. C. Schaefer and G. A. Peters, *J. Org. Chem.*, 1961, **26**, 2778.
- 30 R. Gleiter, E. Heilbronner and V. Hornung, *Helv. Chim. Acta*, 1972, **55**, 255.
- 31 H. Kato, K. Hirao and K. Yamashita, *J. Mol. Struct.*, 1982, **88**, 265.
- 32 B. M. Peake, P. H. Rieger, B. H. Robinson and J. Simpson, *J. Am. Chem. Soc.*, 1980, **102**, 156; P. H. Rieger, *J. Magn. Reson.*, 1982, **50**, 485; J. A. De-Gray and P. H. Rieger, *Bull. Magn. Reson.*, 1986, **8**, 95.
- 33 C. J. Rhodes and M. C. R. Symons, *J. Chem. Soc., Chem. Commun.*, 1989, 1393.

Paper 2/01771G

Received 30th March 1992

Accepted 16th June 1992